Dynamic density functional study of a driven colloidal particle in polymer solutions

F. Penna,[1] J. Dzubiella,[2] and P. Tarazona[1]
[1]*Departamento de Física Teórica de la Materia Condensada, Universidad Autónoma de Madrid, E-28049 Madrid, Spain*
[2]*University Chemical Laboratory, Lensfield Road, Cambridge CB2 1EW, United Kingdom*
(Received 25 September 2003; published 30 December 2003)

The dynamic density functional (DDF) theory and standard Brownian dynamics simulations (BDS) are used to study the drifting effects of a colloidal particle in a polymer solution, both for ideal and interacting polymers. The structure of the stationary density distributions and the total induced current are analyzed for different drifting rates. We find good agreement with the BDS, which gives support to the assumptions of the DDF theory. The qualitative aspect of the density distribution are discussed and compared to recent results for driven colloids in one-dimensional channels and to analytical expansions for the ideal solution limit.

DOI: 10.1103/PhysRevE.68.061407 PACS number(s): 82.70.Dd, 05.70.Ln, 61.20.−p

I. INTRODUCTION

Mixtures of colloids and nonadsorbing polymer coils have attracted much attention over the past decade both experimentally and theoretically [1]. They provide an excellent model system to understand the generic equilibrium and nonequilibrium physics of multicomponent colloidal mixtures due to the fact that the interactions between the constituents can be tailored [2]. The theoretical approaches to the study of the equilibrium phase behavior of colloid-polymer mixtures were largely based on the Asakura-Oosawa (AO) [3] model, in which the chains are modeled as ideal particles experiencing a hard-core repulsion with the colloids. Recently, extensive computer simulations [4] revealed qualitative differences in the phase diagrams when interactions between the polymers are included. However, the off-equilibrium behavior of these systems is far from being understood. In this paper, we present results based on a recently proposed dynamical density functional (DDF) formalism [5,6] and we demonstrate that the latter is capable of describing out-of-equilibrium diffusive processes at the Brownian time scale. The advantage of the DDF theory is the fact that particle interactions are included once a good approximation for the equilibrium functional is known and it is well suited to treat different external potentials.

The system under consideration is a colloidal particle being dragged at a constant rate c (e.g., by gravitation, electric or magnetic fields, or by optical clamps [7]) through a solution of polymers in a light solvent. The spherical colloid is represented by an external potential $V_{\mathrm{ext}}(\mathbf{r},t)=V_{\mathrm{ext}}(|\mathbf{r}'|)$, where $\mathbf{r}'\equiv\mathbf{r}-ct\hat{\mathbf{z}}$ is the coordinate in the reference framework of the colloidal particle. The solvent provides the rest framework for the Langevin dynamics of the polymers, which have a mobility Γ_0, connected through the Einstein relation to the diffusion constant and the inverse thermal energy, $\beta=(k_BT)^{-1}$. Assuming that the polymer gyration radius and the colloidal particle have similar size, $\sigma \sim 10^{-7}$m, and with the viscosity of a typical solvent at room temperature, the natural units for the shifting rate $\Gamma_0/(\beta\sigma)$ would be in the range of 10^{-4}m/s, and we may safely neglect the hydrodynamic effects of the light solvent. The much heavier globular polymers would feel the competing effects of the solvent, as rest framework for their Brownian dynamics, and the moving colloidal particle drifts with respect to the polymers at a constant rate (drift velocity) c. The deterministic DDF theory [5,6] is an extension of the density functional (DF) formalism to off-equilibrium systems, which includes exactly the ideal gas and the external potential contributions to the free energy, and it represents the correlations out of equilibrium by those of an equilibrium system with the same density distribution. With this hypothesis, and the interpretation of the density $\rho(\mathbf{r},t)$ as the average of the instantaneous density over the random noise in the molecular Langevin dynamics, the theory enables the use of the well developed approximations for the equilibrium Helmholtz free energy in DF theory, which are usually split into the ideal gas and interaction contributions, $\mathcal{F}[\rho]=\mathcal{F}_{\mathrm{ideal}}[\rho]+\Delta\mathcal{F}[\rho]$. The central DDF equation for the time-dependent density distribution is

$$\frac{\partial\rho(\mathbf{r},t)}{\partial t}=\Gamma_0\nabla\left[\rho(\mathbf{r},t)\nabla\left(\frac{\delta\mathcal{F}[\rho]}{\delta\rho(\mathbf{r},t)}+V_{\mathrm{ext}}(\mathbf{r}')\right)\right]. \qquad (1)$$

From any initial distribution of polymers, the time evolution would take the system towards a stationary density distribution $\rho(\mathbf{r},t)=\rho(\mathbf{r}-\hat{\mathbf{z}}ct)\equiv\rho(\mathbf{r}')$, shifting at the same rate c as the external potential. This distribution is the most relevant property of the system and it corresponds to the solution of the functional equation

$$\nabla\cdot\left[\rho(\mathbf{r}')\nabla\left(\frac{\delta\mathcal{F}[\rho]}{\delta\rho(\mathbf{r}')}+V_{\mathrm{ext}}(\mathbf{r}')+\frac{cz'}{\Gamma_0}\right)\right]=0, \qquad (2)$$

where the time dependence is fully adsorbed into the coordinate $\mathbf{r}'$. The solution of Eq. (2) has been explored for systems with one-dimensional (1D) dependence of the potential barrier [8], $V_{\mathrm{ext}}(\mathbf{r}')=V_{\mathrm{ext}}(z')$, along the shifting direction; the similarities and the differences with the Euler-Lagrange equation for the DF theory of equilibrium systems were analyzed there both for ideal and interacting systems. However, the 3D geometry of the present problem requires a different analysis, since the zero-divergence requirement for the brackets in Eq. (2) leaves open a much wider functional space in 3D than in 1D.

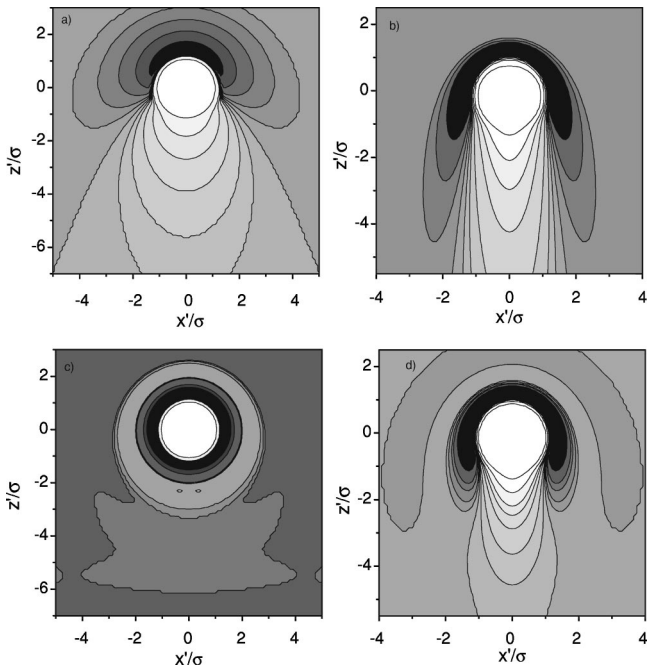

FIG. 1. Steady state contour density field of ideal (a), (b) and interacting (c), (d) polymers created by a driven colloidal particle. Shown is the density in the $x'z'$ plane where the center of the colloid is located. The colloid is moved along the z' axis at a velocity $\sigma\bar{c}=1$ (a), (c) and $\sigma\bar{c}=10$ (b), (d). Bright regions correspond to low densities while dark regions show high densities.

II. NONINTERACTING POLYMERS

Starting in the spirit of the AO model, for noninteracting polymers, $\Delta\mathcal{F}=0$, Eq. (2) becomes a linear Fokker-Planck equation

$$\nabla^2\rho+\nabla(\rho\cdot\nabla\beta V_k)=0, \tag{3}$$

with a "kinetic potential" given by $\beta V_k(\mathbf{r}')=\beta V_{\text{ext}}(\mathbf{r}')+\bar{c}z'$, as a function of the reduced shifting rate $\bar{c}\equiv\beta c/\Gamma_0$ with inverse length units. In Figs. 1(a) and 1(b) we present numerical solutions for the density distribution of the ideal case with bulk density $\rho_0\sigma^3=1$, under the effects of the external potential

$$V_{\text{ext}}(\mathbf{r}')=V_0\exp(-|\mathbf{r}'/\sigma|^6), \tag{4}$$

with $\beta V_0=10$, to represent the soft repulsion between the polymers and the shifting colloidal particle. The bulk density ρ_0 is the value of the density far away from the external potential and is obviously the same both for the equilibrium and the nonequilibrium driven system; moreover, for the ideal noninteracting system ρ_0 just provides an arbitrary factor to $\rho(\mathbf{r}')$.

The density distribution around the external potential $\rho(\mathbf{r}')$ has axial symmetry and exhibits a caplike structure with $\rho(\mathbf{r}')>\rho_0$ in the *front* ($z'\gtrsim\sigma$), formed by the polymers being pushed by the moving repulsive external potential. These particles escape around the colloidal particle creating a skirt for $z'\lesssim-\sigma$, which, together with the hole [$\rho(\mathbf{r}')<\rho_0$] left behind by the potential, form a *wake* structure extending much further than the *front* structure for $z'\gtrsim\sigma$. An increased shifting rate [$\bar{c}\sigma=10$ in Fig. 1(b) compared to $\bar{c}\sigma=1$ in Fig. 1(a)], enhances these characteristics, with a higher density front and a narrower skirt reaching further away behind the shifting colloidal particle.

The transverse integral of $\rho(\mathbf{r}')-\rho_o$ over $x'y'$ plane as function of z' gives an excess of polymers in the front region but it vanishes in the wake region, as the positive wings exactly compensate the depletion close to the z' axis. This is reminiscent of the 1D result [8] for a shifting repulsive barrier with a front density $\rho(z')=\rho_0+A\exp(-\bar{c}z')$ and no wake, $\rho(z')=\rho_0$, behind. The absence of excess molecules in the wake seems to be a generic characteristics of stationary states under constant bulk boundary conditions with purely relaxative dynamics of the ideal gas molecules. Using cylindrical coordinates $\mathbf{r}'=(R,\phi',z')$ we now explore analytically the asymptotic forms of both the front and the wake regions, where $V_{\text{ext}}(r')=0$ reduces Eq. (2) to

$$\frac{1}{R}\frac{\partial}{\partial R}\left(R\frac{\partial\rho(\mathbf{r}')}{\partial R}\right)+\frac{\partial^2\rho(\mathbf{r}')}{\partial z'^2}+\bar{c}\frac{\partial\rho(\mathbf{r}')}{\partial z'}=0. \tag{5}$$

Through a Hankel transform, the solution for the cylindrically symmetric $\rho(\mathbf{r}')$ is

$$\rho(R,z')=\rho_0+\int_0^\infty d\alpha\,\alpha\,f(\alpha)J_0[\alpha R]e^{-\beta z'}, \tag{6}$$

where $\beta_\pm=\bar{c}/2\pm\sqrt{(\bar{c}/2)^2+\alpha^2}$ and J_0 is the zeroth-order Bessel function. Far away from the external potential, a fast convergence of the Hankel components $f(\alpha)$ is observed, and the relevant features come from their behavior for $\alpha\ll\bar{c}$. Hence we may use $\beta_+\approx\bar{c}+\alpha^2/\bar{c}$ and $\beta_-\approx-\alpha^2/\bar{c}$, for the front and the wake regions, respectively. The expansion of $f_\pm(\alpha)$ as an even polynomial function for small α and the zero wake requirement lead to $f_-(\alpha)\approx A_1\alpha^2+A_2\alpha^4+\cdots$ in the wake, while at the front we expect $f_+(\alpha)\approx B_0+B_1\alpha^2+B_2\alpha^4+\cdots$. Thus

$$\rho(R,z')\approx\rho_0+e^{-\bar{c}z'}e^{-a^2/4}\left[B_0\frac{w^2}{2}+B_1\frac{w^4}{8}(a^2-4)+B_2\frac{w^6}{32}(a^4-16a^2+32)+\cdots\right] \tag{7}$$

for $z'\gg\sigma$, and

$$\rho(R,z')\approx\rho_0+e^{-a^2/4}\left[A_1\frac{w^4}{8}(a^2-4)+A_2\frac{w^6}{32}(a^4-16a^2+32)+\cdots\right], \tag{8}$$

for $z'\ll-\sigma$, where $w=\sqrt{\bar{c}/|z'|}$ and $a=wR$.

Although the amplitudes of these contributions depend on the particular external potential, the asymptotic decay forms are generic. For a fixed z', the structure in the transverse plane is given by a Gaussian times a polynomial function. In

our case the positive values of A_1 and B_0 lead to a maximum front density at $R=0$, while the leading term at the wake gives a minimum at $R=0$ and maximum at $R=2^{3/2}\sqrt{|z'|/\bar{c}}$, producing the caplike structure with parabolic shape shown in Figs. 1(a) and 1(b). Besides the lack of A_0, the qualitative difference between the advancing front and the wake comes from the exponential decay, $\exp(-\bar{c}z')$, behavior of the front, which restricts the density structure to the neighborhood of the external potential, as in the $1D$ result, while for fixed a the wake structure decays as inverse powers of z', with a $1/z'^2$ leading term. We have tested these analytical predictions with the numerical solution of Eq. (2), and got quantitative agreement for $z'>1.25\sigma$ ($\bar{c}\sigma=10$) and $z'>3\sigma$ ($\bar{c}\sigma=1$) in the front region, and $z'<-7\sigma$ in the wake region for any $\bar{c}$. The contributions from higher-order terms in Eq. (8) appear to be more important than in Eq. (7), although the qualitative aspect of the wake is already well represented by the first term in Eq. (8).

Nevertheless, we have to point that, contrary to the 1D case [8], the front and the wake regions in our 3D system are in fact connected through the regions, with small $|z'|$ but large R, were the external potential created by the shifting colloidal particle on the polymers vanishes; so that the solution of Eq. (5) should have a unique analytic form, common to the front and the wake region. This has the obvious difficulty of using both the positive (β_+) and the negative (β_-) decay constants for the positive (front) and negative (wake) values of z', leading to exponential growth of their respective contributions, which may only be canceled by the appropriate behavior of $f(\alpha)$ for large α, beyond the Taylor expansion used in Eqs. (7) and (8). The good comparison of our numerical solutions with the analytic results, Eq. (7) for the front and Eq. (8) for the wake reflects a local asymptotic convergence which is quite useful to understand the qualitative features of the stationary density distribution, but which cannot be taken as an exact global asymptotic result. It has to be pointed that the use of spherical, rather than cylindrical coordinates to solve Eq. (6) also leads to problems of convergence, as the parabolic structure of the wake implies the entanglement of the radial and the angular coordinates.

III. THE EFFECT OF POLYMER INTERACTION

For the case of interacting polymers the steric effects lead to an effective repulsion between them, which we model by the ultrasoft Gaussian pair potential [11–16]

$$\phi(r_{ij})=U_0\exp(-r_{ij}^2/\sigma^2), \tag{9}$$

where r_{ij} is the interparticle distance and $\beta U_0=1$. Both for equilibrium [12–15] and dynamical properties [17] the excess free energy density functional of this model has been successfully approximated by a pure *mean field* [or random-phase approximation (RPA)] form

$$\Delta\mathcal{F}[\rho]=\frac{1}{2}\int d^3\mathbf{r}\int d^3\mathbf{r}'\,\phi(|\mathbf{r}-\mathbf{r}'|)\rho(\mathbf{r})\rho(\mathbf{r}'). \tag{10}$$

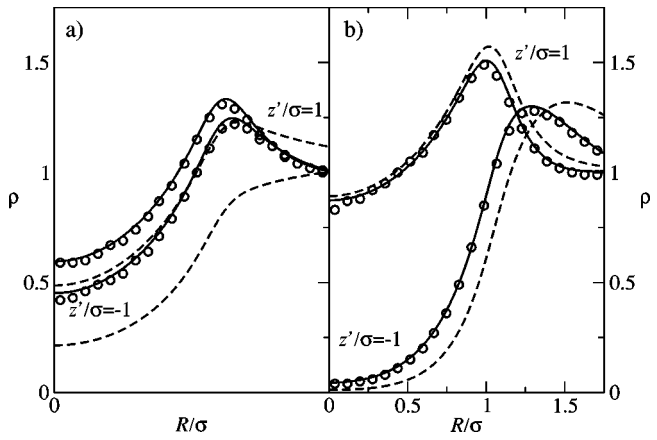

FIG. 2. Steady state density profiles of the polymers around a driven colloid at $z'/\sigma=0$ plotted as a function of the radial distance R/σ from the z' axis for fixed $z'/\sigma=\pm1$. The shifting rates are (a) $\sigma\bar{c}=1$ and (b) $\sigma\bar{c}=10$. Dashed lines are the results for ideal polymers, while the curves for interacting polymers are plotted with solid lines. The symbols (circles) are the simulation results.

Instead of solving the integro-differential Eq. (2) with this model, we have obtained the steady state distribution by the time integration of Eq. (1) from a uniform density initial state. The stationary structure around the colloidal particle are reached with short integration times, as presented in Fig. 1 for $\rho_0\sigma^3=1$ (which represents a fairly dense polymer solution) and $\bar{c}=1\sigma$ (c) and $\bar{c}=10\sigma$ (d). At the low velocity $\bar{c}\sigma=1$ the influence of interactions between the polymers is very strong. The spherical layering structure created around the colloidal particle by the polymer-polymer repulsion is much stronger than the front-wake asymmetry induced by the dragged colloid; the extension of the wake behind the moving particle is strongly reduced by the much lower bulk osmotic compressibility of the interacting system, which facilitates the filling of the axial hole by radial currents. At the higher $\bar{c}\sigma=10$ shifting rate in Fig. 1(d) the effects of the interactions are much weaker. Although there is still a clear shortening of the wake, explained by the lower osmotic compressibility, the main qualitative change with respect to the ideal solution result in Fig. 1(b) is that the layering created by the packing effects produces a double cuplike structure, reaching further away from the z'-axis.

In Fig. 2 we present a quantitative view of our results; we plot the polymer density as a function of the distance R to the z' axis for fixed values of $z'/\sigma=\pm1$. The solution of the DDF approach is compared to standard BDS [18]. Here, the stochastic Langevin equations for the overdamped colloidal motion of N particles with trajectories $\mathbf{r}_i(t)$ $(i=1,\ldots,N)$ read as

$$\Gamma_0^{-1}\frac{d\mathbf{r}_i}{dt}=-\nabla_{\mathbf{r}_i}\sum_{j\neq i}\phi(|\mathbf{r}_i-\mathbf{r}_j|)+\mathbf{F}_{\rm ext}(t)+\Gamma_0^{-1}c\hat{\mathbf{z}}+\mathbf{F}_i^{(\rm R)}(t). \tag{11}$$

There are different forces acting onto the colloidal particles: first there is the force attributed to interparticle interactions, second there is the external field $\mathbf{F}_{\rm ext}$ due to the colloidal

particle, $\Gamma_0^{-1}\mathbf{c}$ is the driving force, and finally the random forces $\mathbf{F}_i^{(\mathrm{R})}$ describe the kicks of the solvent molecules acting onto the ith colloidal particle. These kicks are Gaussian random numbers with zero mean, $\overline{\mathbf{F}_i^{(\mathrm{R})}}=0$, and variance

$$\overline{(\mathbf{F}_i^{(\mathrm{R})})_\alpha(t)(\mathbf{F}_j^{(\mathrm{R})})_\beta(t')}=2k_BT\Gamma_0\delta_{\alpha\beta}\delta_{ij}\delta(t-t'). \quad (12)$$

The subscripts α and β stand for the three Cartesian components. The simulations were carried out with $N=1000$ particles, periodic boundary conditions in all directions and box sizes $L_x=L_y=8\sigma$ and $L_z=16\sigma$. After an equilibration time of 10^5 time steps, statistics were gathered over a period of 2×10^6 time steps. In both, simulation and numerical solution of the DDF, the density is averaged over rings at z' and radius R with a cross section $\sigma^2/4$.

The good agreement between the BDS data and the DDF results gives support to both the mean field approximation (10) used to describe the effect of the interactions, and to the DDF borrowing of the equilibrium intermolecular forces, as functionals of the instantaneous density distribution [5,6]. The comparisons between the ideal solution and the interacting system shows again that the polymer interactions affect much more the features of the density distribution for low $\bar{c}$ than for high $\bar{c}$. For $\bar{c}\sigma=1$ the polymer layer around the colloidal shows only a slight asymmetry for $\sigma\gtrsim z'\gtrsim-\sigma$, while the kinetic effects in ideal gas create a maximum at the front $z'\gtrsim\sigma$.

Qualitatively we may associate the behavior of the front structure to the direct kinetic effect of the advancing spherical repulsive potential created by the colloidal particle. As c grows the kinetic constrain on their Brownian trajectories becomes the dominant factor for the movement of the polymers at the front. The polymer-polymer interaction plays then a minor role, so that for $\bar{c}\sigma\gg1$ the main peak in the front structure becomes similar for ideal and interacting polymers. The structure of the wake is determined by the diffusion from the bulk solution to fill the void left behind the colloidal particle, the effect of the higher osmotic pressure accelerates that process and produces a weaker wake than in the ideal solution limit. On the opposite extreme, for very low shifting rates of the colloidal particle, the effects of the polymer-polymer interactions are very important, both at the front and at the wake structures. At high polymer concentrations the structure around the colloidal particle is dominated by the steric repulsions between polymers. The relatively rigid structure of molecular layers is shifted, with little deformations, by the moving colloidal particle.

IV. DISCUSSION

As the first point in our discussion, we consider the total excess of polymers ΔN, produced by $V_{\mathrm{ext}}(\mathbf{r}')$ over the uniform bulk density.This is a relevant data since $c\Delta N$ is the total polymer current, which requires a total force $c\Gamma_o\Delta N$ provided by the colloid on the polymers. There is a generic DDF relation

$$\Delta N\equiv\int d^3\mathbf{r}'[\rho(\mathbf{r}')-\rho_o]=-\frac{\beta}{\bar{c}}\int d^3\mathbf{r}'\rho(\mathbf{r}')\frac{\partial V_{\mathrm{ext}}(\mathbf{r}')}{\partial z'}$$

for the stationary density distributions, which allows to calculate the total excess from the density distribution in the neighborhood of the external potential. The results for the systems in Fig. 1 are: $\Delta N_a=3.05$, $\Delta N_b=1.883$, $\Delta N_c=2.53$, and $\Delta N_d=1.879$. Again, the difference between the interacting and the ideal cases is strongly reduced at $\bar{c}\sigma=10$, with respect to $\bar{c}\sigma=1$. It is remarkable that the static equilibrium result for ΔN in the ideal gas case would be negative [as $\rho(\mathbf{r})=\rho_o\exp(-\beta V_{\mathrm{ext}}(\mathbf{r}))\leqslant\rho_o$], but the stationary excess ΔN is positive and grows as c decreases. This may be understood from the analytical 1D result [8] for the front $\rho(z')-\rho_o\sim c\exp(-\bar{c}z')$, which vanishes locally as $c\to0$, but it still gives a positive integral that overcompensates the depletion inside the potential barrier and produces $\Delta N>0$, consistently with the sign (and value) of the total force. The difference between the equilibrium ($c=0$) density distribution and that of a stationary state at arbitrarily small but positive $\bar{c}$ is remarkable. The apparent paradox come from the concept of stationary state, which would appear after a short transient period when $\bar{c}$ is large, but it would require diverging times as $\bar{c}\to0$. The very weak but extended structure of the exponential front in $\rho(\mathbf{r}')$ for $\bar{c}\sigma\ll1$ would never be observed in practice, and the transient states $\rho(\mathbf{r},t)$ for any reasonable t would be very similar to the equilibrium structure for $c=0$. Nevertheless, the strongly anisotropic density distributions, with nontrivial global effects even for very low $\bar{c}$, suggest important effects on the interaction between two driven colloids in a bath of quiescent Brownian particles [19], qualitatively different from effective interactions in equilibrium [1,9,10].

Finally we comment on the relevance of the boundary conditions and the system dimension by comparing the present results with the 1D system explored in a previous work [8]. Obviously, in the system explored here the effects on the bulk polymer solution are limited to the neighborhood of the single colloidal particle. If we consider a finite concentration of colloidal particles, all being drifted at the same rate c with respect to the stationary framework of the solvent, there would be a finite induced polymer current per unit volume. The 3D structure, which offers easy paths for the polymers to escape from the colloidal particles, would probably make unfeasible the approach to the full-drift regime discussed for 1D systems, in which nearly all the particles move along the shifting potential. Another possible problem in 3D which may be of interest are currents through a structured barrier with holes or slits. However, we have to be aware of the intrinsic limitations of our DDF approach, particularly in the treatment of the solvent as an inert reference framework for the Langevin dynamics of the polymers, which is not affected by the shifting external potential (or colloidal particle). Altogether, we may conclude that the DDF offers a good theoretical tool to explore dynamical problems in polymers solutions subject to time-dependent

external potentials which do not affect the solvent, and the formalism may also be used to predict, in good agreement with BDS, the density structures created around colloidal particles or similar sized molecules moving slowly with respect to the solvent. However, the extension to problems in which the solvent plays a more direct role should be regarded with caution, as they may require a more symmetrical treatment of the solute and the solvent.

ACKNOWLEDGMENTS

We are grateful to R. Roth for helpful comments. This work was supported by the Dirección General de Investigación Científica (MCyT) under Grant No. BMF2001-1679-C03-02, and a FPU Grant No. AP2001-0074 from the MECD of Spain. J.D. acknowledges the financial support of EPSRC within the Portfolio Grant No. RG37352.

[1] W.C.K. Poon, J. Phys.: Condens. Matter **14**, R859 (2002).
[2] P.N. Pusey, in *Liquids, Freezing and the Glass Transition*, edited by J.-P. Hansen, D. Levesque, and J. Zinn-Justin (North Holland, Amsterdam, 1991).
[3] S. Asakura and F. Oosawa, J. Chem. Phys. **22**, 1255 (1954).
[4] P.G. Bolhius, A.A. Louis, and J.-P. Hanson, Phys. Rev. Lett. **89**, 128302 (2002).
[5] U. Marini Bettolo Marconi and P. Tarazona, J. Chem. Phys. **110**, 8032 (1999).
[6] U. Marini Bettolo Marconi and P. Tarazona, J. Phys.: Condens. Matter **12**, A413 (2000).
[7] A.P. Philipse, Curr. Opin. Colloid Interface Sci. **2**, 200 (1997); D.G. Aarts, J.H. van der Wiel, and H.N.W. Lekkerkerker, J. Phys.: Condens. Matter **15**, S245 (2003); P. Wette *et al.*, J. Chem. Phys. **114**, 7556 (2001).
[8] F. Penna and P. Tarazona, J. Chem. Phys. **119**, 1766 (2003).
[9] J.-P. Hansen and H. Löwen, in *Bridging Time Scales: Molecular Simulations for the Next Decade* (Springer, Berlin, 2002), pp. 167–198.
[10] C.N. Likos, Phys. Rep. **348**, 267 (2001).
[11] F.H. Stillinger, J. Chem. Phys. **65**, 3968 (1976).
[12] A.J. Archer and R. Evans, Phys. Rev. E **64**, 041501 (2001).
[13] A.J. Archer and R. Evans, J. Phys.: Condens. Matter **14**, 1131 (2002).
[14] A. Lang, C.N. Likos, M. Watzlawek, and H. Löwen, J. Phys.: Condens. Matter **12**, 5087 (2000).
[15] A.A. Louis, P.G. Bolhuis, and J.-P. Hansen, Phys. Rev. E **62**, 7961 (2000).
[16] A.A. Louis, P.G. Bolhuis, J.-P. Hansen, and E.J. Meijer, Phys. Rev. Lett. **85**, 2522 (2000).
[17] J. Dzubiella and C.N. Likos, J. Phys.: Condens. Matter **15**, L147 (2003).
[18] M.P. Allen and T.J. Tildesley, *Computer Simulation of Liquids* (Clarendon Press, Oxford, 1989).
[19] J. Dzubiella, C. N. Likos, and H. Löwen Phys. Rev. Lett. (to be published), e-print cond-mat/0306069.